Behaviour of Ferrocement Sandwich Panels Slabs under Shear

Yousry B. Shaheen[1], Amal A. Nasser[1,c] and Wesam S. El-Habashy[1]

[1]Civil Engineering Department, Faculty of Engineering, Minufiya University, EGYPT

Abstract

A sandwich panel consists of two thin skin layers of ferrocement layers; separated by a thick layer of polystyrene core. This type is considered a light weight building materials section. Effect of silica fume on concrete properties was investigated to determine the optimum percentage of silica fume as cement replacement. Twelve composite slabs 120cm*120cm and 14cm thick were cast. Light weight composite slabs were subjected to central load. The use of metal mesh was proposed as a viable alternative to ordinary steel bars in reinforcing ferrocement plates. Additional mild steel bars were used with steel mesh to enhance the mechanical behaviour of the composite slab. Using lightweight materials lead to decrease the weight of structural member's and consequently decrease the overall dead load of the building. The study included comparisons between flexural strength, crack pattern, first crack load, and deflection under different stages of loading of the tested sandwich panels.

Keywords: Ferrocement; Sandwich Panels; Light Weight; Composite Section; Steel Mesh.

1.   Introduction

Using ferrocement laminates for repairing cracked reinforced concrete columns was introduced by Fahmy et al. in 1999 [1]. In 2004, Fahmy et al. conducted a research on the ferrocement panels for use as floor units. Ferrocement sandwich panels and hollow core panels were developed to be investigated as flexural slabs. For sandwich panels developed, two types of core materials were investigated: the light brick core and foam concrete [2]. Ferrocement behaves like conventional reinforced concrete in its load bearing characteristics; however, the main difference is that crack development process is delayed by the dispersion of the reinforcement in fine form through the mortar [3]. Ferrocement sandwich panel is one of the developed applications of Ferrocement technology that offer an ideal building material [4]. A sandwich panel consists of two thin skin layers of relatively high strength and modulus of elasticity, separated by a thick layer of a low strength material as a core. The advantage of this type of building materials is mainly the light weight of the unit compared to its equivalent volume of the conventional concrete. Such panels could be used as roof elements or as wall bearing elements. This is mainly due to the two outer thin skin layers, which can carry loads, resist impacts, and accommodate architectural acceptance, while in the same time the core material provides thermal and sound insulation.

Moreover, the core material can provide shear transfer between the two thin skin layers if the units are to be used for structural or load bearing purposes. In this case, the core material should possess adequate strength to be able to transfer the shear force between the two layers. Ferrocement lightweight sandwich panel system was investigated in previous researches and has proven that it is one of the most suitable structural systems [5].

Few of the many studies of ferrocement have included shear strength evaluation; perhaps because ferrocement is used primarily in thin panels where the span/depth ratio in flexure is large enough that shear is not the governing failure criterion. Parallel longitudinal alignment of the reinforcing layers in ferrocement effectively precludes the inclusion of shear reinforcement equivalent to the bent-up bars or stirrups used in reinforced concrete. So, ferrocement is not particularly suited to resisting shear. However, this is not required in most applications. Shear strength has been determined for specimens reinforced with woven mesh and skeletal bars, tested in bending at a shear span/depth ratio of 0.4-0.55.

While the test values reflect the characteristics of the steel and mortar used, the shear strength remains at a constant fraction of about 32% of the equivalent flexural strength for a fairly wide range of steel contents. Tests conducted in bending on specimens reinforced with welded mesh at span/depth ratios ranging from 1 to 3 indicate that failure in transverse shear is possible for specimens with high volume fraction of reinforcement and low strength of mortar only at a small span-depth ratio. However, shear failure is preceded by the attainment of flexural capacity of ferrocement. In the case of in-plane shear, similar to that existing in the web of an I-beam under transverse loading, the Truss Model Theory has been found to give a good estimate of the ultimate shear strength. The punching shear failure often governs the strength of the footing-to-column connection [3].

Punching shear strength enhancement between 31-53% was obtained with the application of the proposed Carbon Fiber Reinforced Polymer retrofit method. The displacement and the ultimate load capacities of strengthened specimens with rectangular column tended to decrease with respect to strengthen specimens having square column [6, 7]. The combination of steel fibre reinforced concrete and conventional reinforcement has in many researches shown to emphasize good bearing capacity [8]. A new method to increase the strength and ductility of the footing was proposed by inserting the punching shear preventers (PSPs) into the footing. The validation and effectiveness of the proposed method were verified by a series of tests and nonlinear finite element analysis [9, 10]. The strength and ductility of the footing were considerably increased by using the PSPs, since the diagonal shear cracks can be effectively isolated by PSPs. Then, the applied load redistributed to the flexural reinforcing bars [11].

2.   Experimental Program

The experimental program passed through three phases:

- Studying the effect of silica fume on the mortar properties and to determine its optimum replacement percentage
- Determining the mechanical properties of the steel bars and meshes used.
- Studying the ultimate load and flexural behavior of ferrocement lightweight sandwich slabs.

2.1.   Materials Used

2.1.1. Cement

A locally product Ordinary Portland cement (OPC) was used in the mortar matrix. The cement was considered to comply with (ASTM Type I) with a specific surface of 3050 cm^2/gm.

There were 2.35% Retained on Sieve 170. All cement tests were conducted in accordance with ASTM (C150-68) [12].

2.1.2. Fine Aggregates

Clean desert sand having physical and mechanical properties comply with Egyptian Standard Specifications. (ESS.1109/1971) [13]. The sand used is 4.75mm maximum nominal size. According to the Ferrocement Model Code [14], the maximum particle size was limited to D/(N+1), where D is the smaller mesh opening, and N is the number of layers of mesh within the section. The sand used is siliceous material. Fineness Modulus was 2.91 mm.

2.1.3. Superplasticizer

It complies with ASTM C-494 Type A & F [15]. Density is Approximately 1.20 kg/lt. Ph value is 8. It was used to provide the necessary workability needed for the concrete mix.

2.1.4. Water

Tape water was used for mixing and curing procedures.

2.1.5. Silica Fume

Silica Fume used as a partial replacement of the cement. It was delivered in a powder form with a light-grey colour. It gives black slurry when it is mixed with mortar. It is commercially bought as ACC Micro silica Grade complies ASTM (C1240-03) [16]. It has less than 10% Retained on 45 micron sieve. Specific surface is 3200 m^2/gram.

2.1.6. Core Material

One type of core material was used to produce the ferrocement slabs under investigation. Reinforced polystyrene block of density 12 Kg/m^3 and 8 cm thick was employed to provide the core material in-between the two skin ferrocement layers. Foam is an insulating material used on a large scale in the field of construction. Foam is gaseous bubbles surrounded by a liquid or a solid matrix. The matrix connection makes closed matrix. Polystyrene is sold under a trademark "Styropor".

2.1.7. Shear Connectors

Using polystyrene as a filling material, the two ferrocement laminates needed cross connections. A 2 mm diameter galvanized wire formed as U-shape were used. The wires worked as shear connectors to create a composite element working as one unit. The shear connectors' distribution is simulated to the columns stirrups according to the Egyptian Code of Practice. A galvanized steel wire of 2 mm diameter is shaped as a U-section. The U-shaped connector is tied to the steel meshes using steel wire-tying.

2.2. Mortar Matrix Used

For all mixes, mechanical mixer with capacity of 0.05 m^3 was used. The constituent materials were first dry mixed; the water was added and the whole patch was re-mixed in the mixer. Mix properties by weight for the different mixes investigated are given in Table 1.

For studying the properties of mortar matrix, 45 cubes 100 x 100 x 100 mm were used to determine the compressive strength for the different mortar mixes at 3, 7, and 28-days age, 15 prisms (100 x 100 x 500 mm) were tested at 28-days age to determine the flexural strength for the different mortar mixes (3 specimens for each mix). 15 cylinders (200 x 100 mm) were used to determine the splitting tensile strength of different mortar mixes. Fresh mortar properties were measured at different silica fume percentages. The slump was measured of mortar mixes according to ASTM (C 143-89a) [17].

The mortar used for casting slabs was designed to get an ultimate compressive strength at 28-days age of (350 kg/cm^2), 35MPa. The mix proportions by weight were (2: 1) for fine aggregate: cementitious materials. The water- cement ratio was 0.4. Fine aggregate water absorption was 0.9%, the ratio was neglected in the mixing water. Superplasticizer was added to mixing water. There were no added water. Various mixes with different percentages of silica fume were investigated to determine the optimum percentage. A super plasticizer was used with all mixes as 2% of weight of cement and silica fume together to maintain suitable workability.

TABLE 1: FERROCEMENT MORTAR MIX PROPORTIONS BY WEIGHT/M^3.

Mix	S.F %	Sand (kg)	Cement (kg)	Water (kg)	Silica fume (kg)	Super-plasticizer(kg)
M$_1$	0	1412	565		0	
M$_2$	5	1412	540		25	
M$_3$	10	1412	515	225	50	11.3
M$_4$	15	1412	490		75	
M$_5$	20	1412	465		100	

2.3.　　Reinforcement Used

2.3.1.　Reinforcing Steel

Six plain mild steel bar specimens were tested under direct tension. For the steel bars used as a main reinforcement for control plates and ferrocement plates, Young's modulus, yield strength and ultimate strength were measured. The average results of the elastic modulus, yield strength, ultimate strength of steel bars are shown in Table 2.

2.3.2. Steel Meshes

Two types of steel meshes were used. The results of the elastic modulus, yield strength, ultimate strength of steel meshes are shown in Table 2.

TABLE 2: MECHANICAL PROPERTIES OF THE STEEL BARS AND STEEL MESHES USED

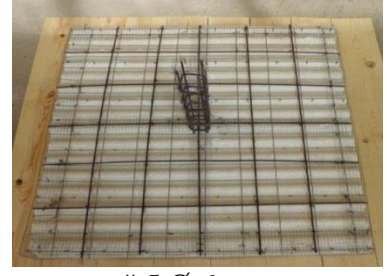| No	Nominal Diameter (mm)	f_Y N/mm^2	f_T N/mm^2	Elon. %	Red. In Area
1	6	277.83	456.74	25.00	68.38 %
2	6	291.99	455.42	31.25	75.01 %
3	6	273.31	454.47	20.00	68.38 %
Mesh type	Proof Stress (N/mm^2)	Proof Strain x 10^{-3}	Ultimate Strength (N/mm^2)	Ultimate Strain x 10^{-3}	
Welded	737	1.17	834	58.8	
Expanded	199	9.7	320	59.2	

2.4.   Ferrocement Sandwich Panels Slabs

In the third phase of the experimental program, 12 simply supported composite light weight ferrocement slabs having the dimensions of 120 x 120 cm and 14 cm thick were tested simply supported along all four sides and subjected to concentrate punching loads acting at columns 120 x 120 cm at the center of slabs. Four designations series, namely A, B, C and D comprise twelve reinforced light weight ferrocement slabs were cast and tested. The details of the four series are shown in Table (3). The top and bottom reinforcement were tied together through welded shear connectors to a rigid cage. The thicknesses of the top and bottom ferrocement skins were kept constant as 30mm. The total thickness of the innovative light weight slab was 14 cm.
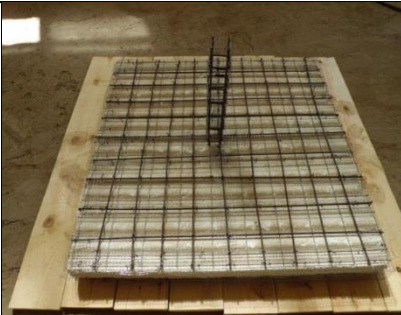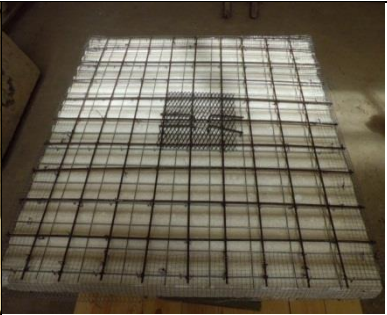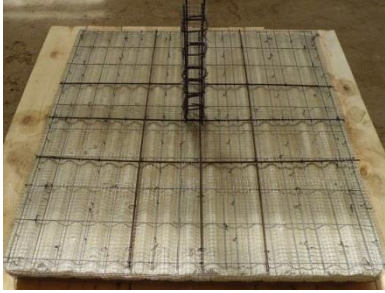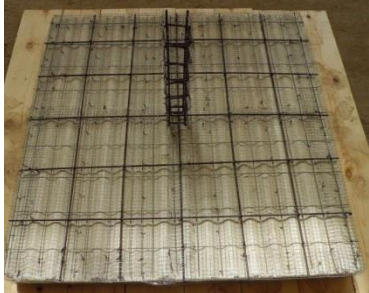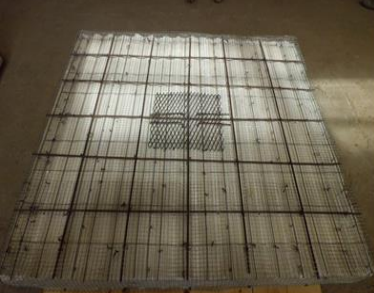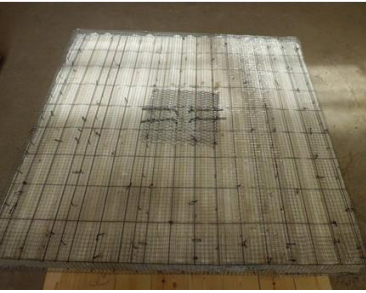
For casting the slabs, a special strong mould was designed. It consisted of 20 mm thick wooded sheet covered with Aluminium thin sheet of 3 mm thick which made observation of cracks during early ages easier. Four Aluminium side angles were screwed to the composite wooden plate with the dimensions required of the specimen.
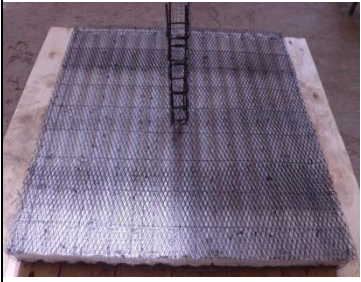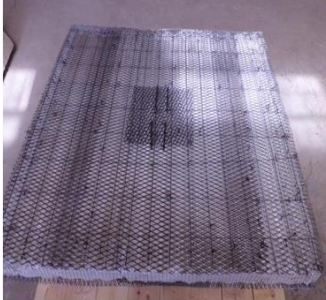
Slabs were tested under central concentrated loadings using hydraulic jack acting on reinforced concrete columns having the dimensions of 12 x 12 cm and 50 cm height. The deflection at each load increment was recorded at center point of the tested slabs. Cracks initiation and their propagations were also observed for each test specimen. The cracking load, deflection at all stages of loadings and ultimate load were measured.

Reinforcement of Ferrocement Sandwich Panel Slabs are shown in Table 3.Volume fraction (V_r) of each slab is calculated, where it is the percentage of reinforcement to the total volume of slab.

TABLE 3:   REINFORCEMENT OF FERROCEMENT SANDWICH PANEL SLABS

Series	Slab No.	V_r. %	Reinforcement	
			Upper part of slab	Lower part of slab
A	**S1**	1.061	# 3 Ø 6 mm	# 3 Ø 6 mm
A	**S2**	1.376	# 5 Ø 6 mm	# 5 Ø 6 mm

A	S3	2.005	 # 9 Ø 6 mm	 # 9 Ø 6 mm
B	S4	1.245	 #3Ø6 mm + one layer welded mesh	 #3Ø6 mm+ one layer welded mesh
B	S5	1.559	 #5Ø6 mm+ one layer welded mesh	 #5Ø6 mm+ one layer welded mesh
C	S6	0.773	 one layer welded mesh	 one layer welded mesh
C	S7	0.956	Two layers welded mesh	Two layers welded mesh
C	S8	1.139	Three layers welded mesh	Three layers welded mesh
C	S9	1.321	Four layers welded mesh	Four layers welded mesh
C	S10	1.5037	Five layers welded mesh	Five layers welded mesh

D	**S11**	1.1003	one layer expanded mesh	one layer expanded mesh
D	**S12**	1.6099	Two layers expanded mesh	Two layers expanded mesh

3.   Test Results and Discussion

3.1.   Properties of Fresh and Hardened Mortar Mixes

Table 4 illustrates the variation of slump and density with increasing the percentage of silica fume. At low replacement percentage of silica fume, 0 % and 5 % silica fume, it was found that mortar consistency was very wet; while at high replacement percentages of 20 % silica fume, mortar became stiff. Constant water-cement ratio and constant super plasticizer percentage used for all mixes irrespective of the silica fume replacement percentage led to the decrease in workability with the increase in silica fume replacement percent, as shown in Table 4. It shows a continuous decrease in density with the increase of silica fume percent.

TABLE 4: EFFECT OF SILICA FUME ON THE PROPERTIES OF FRESH AND HARDENED MORTAR MATRIX.

SF %	Slump (mm)	Density (kg/m^3)	Compressive Strength (MPa)			Splitting Tensile Strength (MPa)	Modulus of Rupture (MPa)
			3d	7d	28days		
0	220	2250	25.5	29.0	37.0	2.2	2.4
5	180	2195	25.0	32.6	41.5	2.3	3.3
10	110	2160	24.2	33.4	48.5	2.7	4.0
15	70	2130	22.9	31.7	44.5	2.4	3.0
20	30	2111	21.9	30.4	41.7	2.3	2.6

The compressive strength increases with the increase in the silica fume replacement up to 10 %, then it decreases with increasing the ratio of silica fume. At 3, 7, 28 days ages, the compressive strength at 10 % replacement with silica fume was higher than that of the other mixes. Therefore, at higher replacement level, there was a significant reduction in strength, where the extra free silica fume did not have enough lime to react with. Slight drop in the early strength up to 7days age compared to the control mix. This may be attributed to the pozzolanic reaction, which took relatively longer time to show effect on strength. The amount of cement was reduced by the replacement percent of silica fume.

The splitting tensile strength at 28 days age for all mixes showed that at 10% replacement gives the highest tensile strength. The increase in the tensile strength up to 10% replacement was

marginally higher than that of the control mix. Similar to compressive strength results, the splitting tensile strength reduced at percentages higher than 10 percent. This was expected as the tensile strength of mortar matrix is always related to its compressive strength. The modulus of rupture of mortar at 28days age was found to be affected by the silica fume percentage in the same manner as the compressive strength. The modulus of rupture for all replacement percentage was found to be higher than that of the corresponding splitting tensile strength.

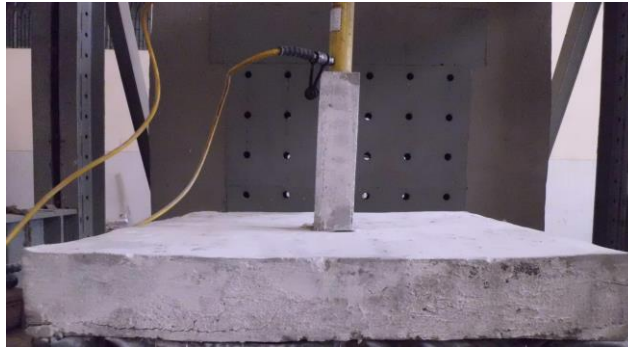## 3.2.   Behavior of Ferrocement Composite Slabs

Figure 1: Test Setup and Applying Load to Test Specimen.

Test rig is shown in Figure 1. It is clear from Figure 2 that using welded steel mesh and expanded steel mesh in reinforcing ferrocement slabs in series designations C and D is effective in increasing their ultimate load than that of steel bar reinforcements for the same volume fraction. Ultimate loads of S4 and S5 (series B) are about 10% higher of Slabs S1 and S2 (series A).

Addition of welded wire mesh improves the slab performance due to the well arrangement of wire meshes with narrow and close spaces, which lead to better bond between the steel mesh and mortar matrix. Consequently, the created stresses due to loading are adequately distributed. The additional steel bars enhanced the behavior under different stages of loading and increased the ultimate carrying capacity of the sandwich panel. Slab S7 (series C, two layers welded galvanized steel mesh and V_r. 0.956%) is approximately equal to that of slab S2 (series A, 5Ø6mm steel bars in both directions, V_r 1.376%). It is significant to enhance the reinforced section by dispersing the reinforcement in the section using steel meshes.

This behavior makes ferrocement more efficient compared to conventional reinforcing materials. The ultimate load of slab S8 (series C, three layers welded galvanized steel mesh at the top and bottom, V_r. 1.139%) is approximately 20 % higher than that of slab S1 (series A, 3Ø6mm steel bars in both directions at the top and bottom). The ultimate load of slab S9 (series C, four layers welded galvanized steel mesh at the top and bottom, V_r. 1.321%) is approximately 18% higher than that of slab S2 (series A, 5Ø6mm steel bars in both directions at the top and bottom, V_r. 1.376%). The ultimate load of slab S10 (series C, five layers welded galvanized steel mesh at the top and bottom. V_r.1.5037%) is 12% higher than that of slab S5 (series B, 5 steel bars Ø 6mm in both directions plus one layer welded galvanized steel mesh, V_r. 1.559%). Therefore, employing galvanized welded steel mesh reached higher strength than that of skeletal steel bars.

Finally comparing the ultimate loads, slab S11 (series D, one layer expanded metal mesh at the top and bottom, V_r. 1.1003%) is 14% higher than that of obtained in slab S1 (series A 3Ø6mm steel bars in both directions at the top and bottom, V_r. 1.061%). The ultimate load of slab S12 (series D, two layers expanded metal mesh at the top and bottom, V_r. 1.6009%) is 8% higher than that of slab S5 (series B, 5 steel bars Ø 6mm in both directions plus one layer welded galvanized steel mesh, V_r. 1.559%).

The Load-Deflection curves of the four series are shown in Figures 3 to 6. It is obvious in all series that increasing the volume fraction of the same reinforcement improves the slab performance
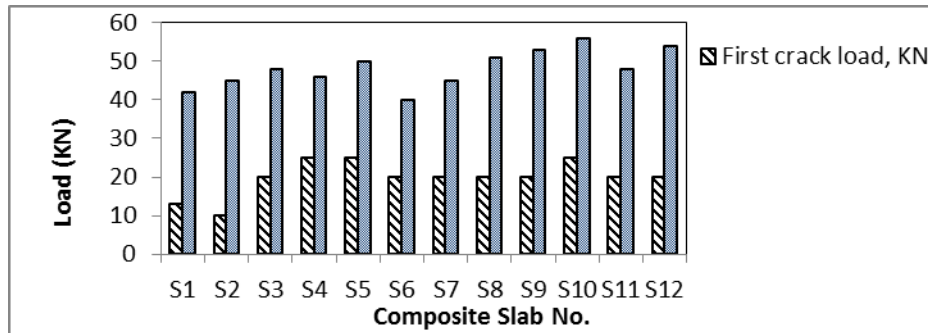

Figure 2: First Crack Load & Ultimate Load of all Ferrocement Slabs.
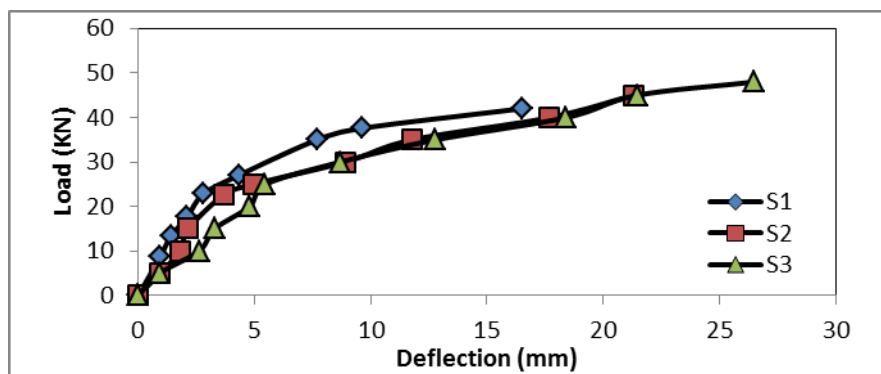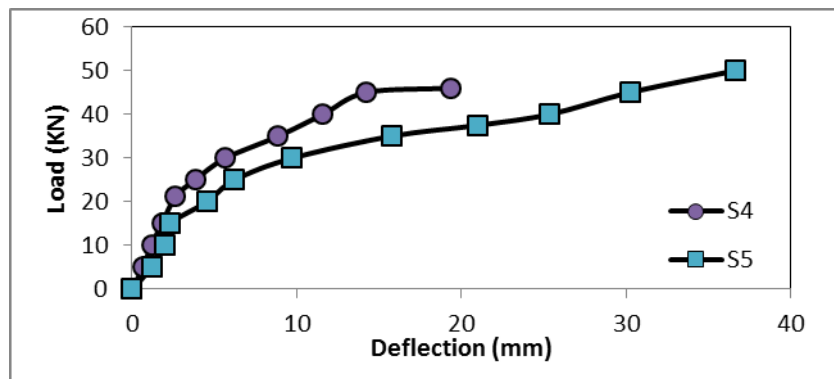

.

Figure 3: Central Load Deflection of Series A.

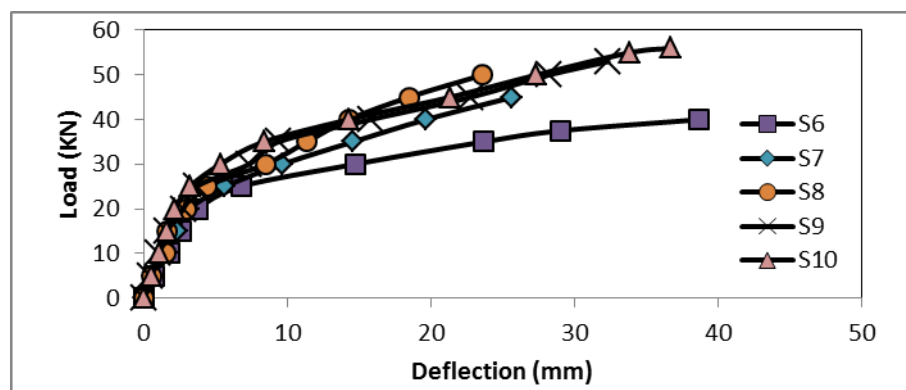

Figure 4: Central Load Deflection of Series B.

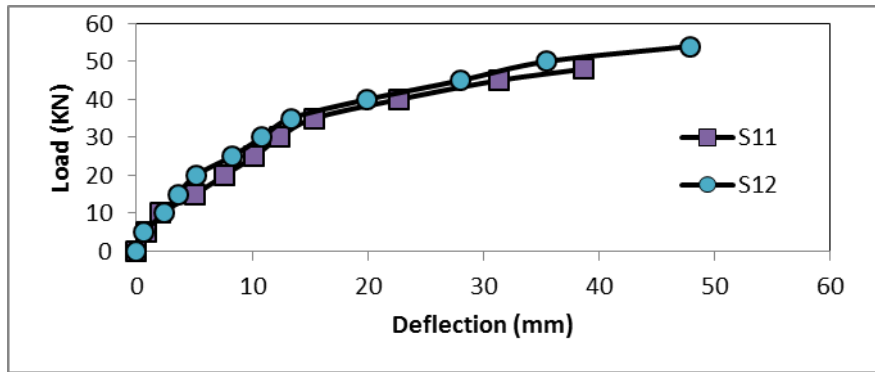Figure 5: Central Load Deflection of Series C.

19

Figure 6: Central Load Deflection of Series D.

Comparisons were made between slabs S2 (series A, 5Ø6mm steel bars in both directions at the top and bottom, V_r. 1.376%) and S9 (series C, four layers welded galvanized steel mesh at the top and bottom, V_r. 1.321%) as shown in Figure 7. Welded wire mesh slab has better performance than that of steel bars reinforcement. It showed higher ductility represented in the area under Load-Deflection curve.

The steel reinforcement dispersion of the wire mesh gives a better distribution of stresses through the loaded section. This volume fraction distribution makes the section acts more likely homogenous. Another comparison was made between slabs S8 (series C, three layers welded galvanized steel mesh at the top and bottom, V_r. 1.139%) and S11 (series D, one layer expanded metal mesh at the top and bottom, V_r. 1.1003%). Although Slab S11 has less ultimate load, it has bigger area under Load-Deflection curve.

The manufacture of the expanded wire mesh makes a better dispersion of the volume fraction. Rhombus shape of expanded mesh transfers stresses through small sections of the mesh material, which has monolithic reinforcement dispersion in the section. The stress transfer of the welded mesh goes through the welded connections, which decrease the wires section during the manufacture process. Crack pattern of the tested slabs are shown in Figure 8. The relative good dispersion of both steel bars and meshes reinforcement decreases the undesired sudden failure of shear. Figure 9 shows the cracking pattern of tested slabs.
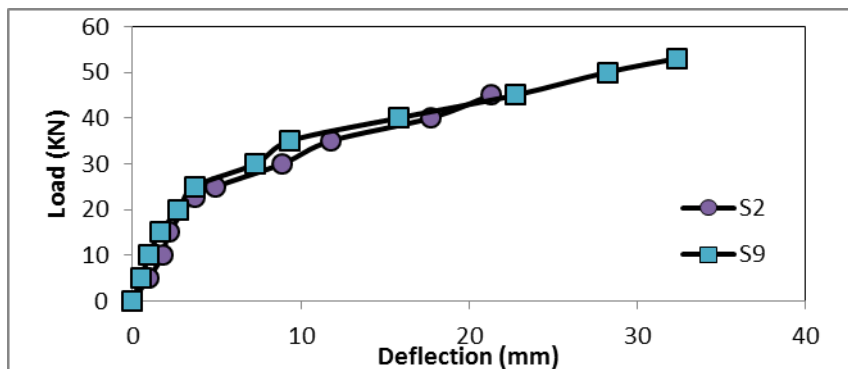

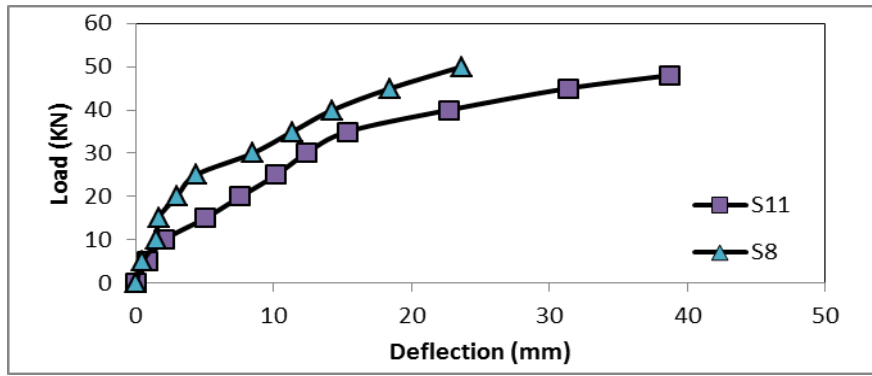Figure 7: Comparison of Central Load Deflection for S2 & S9.

Figure 8: Comparison of Central Load Deflection for S8 & S11.

Figure 9: Cracking Pattern of Tested Slabs.

4. Conclusions

Based on the results and observations of the experimental study presented, the following conclusions could be drawn as follows:

1. Both workability and density of mortar mixes were found to be decreased with the increase of the replacement percentage of silica fume.
2. At all levels of cement replacement, the early age strength was lower than that of control mix strength up to 7days age since the pozzolanic reaction of silica fume takes relatively longer time to show effect on strength.
3. Optimum silica fume percentage as cement replacement was found to be 10% based on the results of both compressive and tensile testes.
4. The effect of silica fume on the flexure strength was found to have similar trend to that of the compressive strength.
5. The developed composite ferrocement slabs emphasized better deformation characteristics and higher cracking and ultimate loads.
6. Irrespective of reinforcement schemes, using welded steel mesh in reinforcing slabs and tying the top and bottom reinforcement into rigid cage with shear connectors going through polystyrene block core resulted in increased ultimate shear punching load of the composite slab.
7. The volume fraction of reinforcing materials used has a great influence on the amount of gain in the resisting moment, ductility and energy absorption. The higher the steel ratio; the higher the gain in the ultimate moment.
8. There is a great saving of weight by employing lightweight composite slabs leading to easy construction especially for weak soil foundations.
9. The developed innovative composite slabs are lighter in weight by compared to conventional concrete slabs in addition to high strength gain.

Among the wide applications that may be of great benefit of light weight slabs investigated is the flexible shaping of roofing such as domes and shells. The construction of light weight slabs may take less time than that of conventional concrete.

References

1. Fahmy, E. H.; Shaheen, Y.B.; and Korany, Y.S., Repairing Reinforced Concrete Columns Using Ferrocement Laminates, Journal of Ferrocement: (1999) Vol. 29, No. 2, pp. 115-124.
2. Fahmy, E. H.; Shaheen, Y. B.; and Abou Zeid, M. N., Development of Ferrocement Panels for Floor and Wall Construction, 5th Structural Specialty Conference of the Canadian Society for Civil Engineering, (2004) June 2-5.
3. American Concrete Institute, ACI Committee 549-1R-88. Guide for the design, construction, and repair of ferrocement. *Manual of Concrete Practice*, Framington Hill, Michigan, USA. (2006). 549.1R-1-549.1R-30.
4. Naaman, A.E. (2000) Ferrocement and laminated cementitious composites. Michigan: Techno Press.
5. Fahmy, E. H.; Shaheen, Y. B.; and Abou Zeid, M. N., Ferrocement Sandwich and Cored Panels for Floor and Wall Construction. Proceedings of the 29th Conference on Our World in Concrete & Structures (2004), 245-252.

6. Bin Mu and Christian Meyer, "Bending and Punching Shear Strength of Fiber-Reinforced Glass Concrete Slabs", ACI Materials Journal, 2003, Volume: 100, Issue: 2, pages(s): 127-132.

7. Tazaly, Z., Punching Shear Capacity of Fibre Reinforced Concrete Slabs with Conventional Reinforcement, MSc. Thesis (2011), Royal Institute of Technology, Stockholm, Sweden

8. Lee, S.; Moon, J.; Park, K.; and Bae K.; Strength of Footing with Punching Shear Preventers, Scientific World Journal (2014) Volume, 15p

9. Wosatko, A.; Pamin, J.; Polak, M.A., Application of Damage–Plasticity Models in Finite Element Analysis of Punching Shear, Computers and Structures Journal (2015), Vol.151, , pp.73–85.

10. Shah, A.A., Applications of Ferrocement in Strengthening of Unreinforced Masonry Columns, International Journal of Geology, Issue 1, Volume 5 (2011), pp.21-27.

11. Subramanian, N., "Alternative Punching Shear Reinforcement for RC Flat Slabs", The Indian Concrete Journal, January (2014), pp. 33-44.

12. Standard Specifications for Portland cement, ASTM (C150).

13. Egyptian Standard Specifications. (ESS.1109/1971).

14. Ferrocement Model Code, Reported by IFS Committee 10, January 2001; (c) Commentary.

15. Standard Specification for Chemical Admixtures for Concrete ASTM (C 494/C 494M – 99)

16. Standard Specification for Use of Silica Fume as a Mineral Admixture in Hydraulic-Cement Concrete, Mortar, and Grout ASTM (C1240)

17. Standard Test Method for Slump of Hydraulic-Cement Concrete ASTM (C 143/C 143M)